

Microstructural Study of Common Concrete Manufactured in Congo-Brazzaville

Jarlon Brunel Makela^{1,2}, Christ Ariel Malanda Ceti¹, Roland Dodji Sodjinou^{1,2},
Nice Ngouallat Mfoutou¹, Narcisse Malanda^{1,2*}

¹Laboratory of Mechanics, Energy and Engineering, Higher National Polytechnic Institute, Marien NGOUABI University, Brazzaville, Republic of the Congo

²Higher Institute of Architecture, Building Planning and Public Works, DENIS SASSOU NGUESSO University, Kintélé, Republic of the Congo

Email: *nar6malanda@gmail.com

How to cite this paper: Makela, J.B., Ceti, C.A.M., Sodjinou, R.D., Mfoutou, N.N. and Malanda, N. (2026) Microstructural Study of Common Concrete Manufactured in Congo-Brazzaville. *Open Journal of Civil Engineering*, **16**, 37-59.
<https://doi.org/10.4236/ojce.2026.161003>

Received: September 24, 2025

Accepted: February 8, 2026

Published: February 11, 2026

Copyright © 2026 by author(s) and Scientific Research Publishing Inc. This work is licensed under the Creative Commons Attribution International License (CC BY 4.0).

<http://creativecommons.org/licenses/by/4.0/>



Open Access

Abstract

This study aims to fundamentally analyze the microstructure of concrete formulated from local materials collected in Brazzaville and Pointe-Noire, developing eight distinct concrete formulations. The objective of this work is to evaluate how the specific composition of each concrete formulation influences the porous structure, which plays a key role in the overall performance of the material, particularly its durability against environmental aggressions. The pore size, which ranges from a few tenths of an angstrom to several microns, illustrates the great microstructural diversity present in these concretes. This diversity is essential to understand, as it directly affects properties such as mechanical strength, permeability to water or chemicals, and the concrete's ability to resist cracking or the penetration of corrosive substances. The precise distribution of these pores thus makes it possible to anticipate the behavior of the material under real conditions of use. To this end, scanning electron microscopy (SEM) was used to observe the size and distribution of pores at different scales, ranging from $\times 100$ to $\times 1000$. This technique offers high resolution, enabling detailed images of the microstructure to be obtained, particularly on fractured and polished samples. The study also highlights the heterogeneous spatial distribution of pores, indicating that the microstructure is not uniformly distributed throughout the sample. This heterogeneity can influence crack propagation, the diffusion of corrosive agents, or overall mechanical strength. Understanding this spatial organization is therefore crucial for the geometric reconstruction of the porous structure, enabling improved modelling and prediction of concrete durability under different conditions of use.

Keywords

Concrete, Microstructures, Electron Microscopy, Pores, Mechanical Strength

1. Introduction

The behaviour of concrete as a construction material requires consideration of the appropriate physical and mechanical properties of its constituents. This assumption provides a better understanding of the internal mechanisms within the cement matrix.

A thorough understanding of the microstructure of concrete is fundamental and essential for optimizing its intrinsic properties, such as compressive strength, tensile strength, toughness and durability against external aggressions. In this regard, many researchers in the fields of civil engineering and materials science have devoted a significant part of their work to the detailed study of microstructure, highlighting the importance of the distribution of aggregates, their size, shape, and the spatial organization of the pores present in the material. Philippi (1994) [1] highlighted the extremely varied range of pore sizes in concrete, ranging from a few tenths of an angstrom to several microns. This diversity directly influences not only the mechanical strength of concrete but also its permeability, *i.e.* its ability to allow water or other degrading agents to pass through.

However, poor formulation of cemented granular materials can create preferential pathways for the migration of pollutants from the surrounding environment, thereby compromising the durability of the material [2].

Given that concrete, after hardening, forms a compact and heterogeneous granular structure, it is essential to study its microstructure in order to better understand the distribution and connectivity of pores, as well as the density of the granular stacking. These elements are essential for predicting the rheological behavior of concrete and anticipating its permeability, resistance to the diffusion of harmful substances, and longevity when used in exposed environments [3] [4]. Our study is part of this approach, analyzing the microstructure of common concretes formulated from local materials in the cities of Brazzaville and Pointe-Noire. The objective of this study is to characterize the microstructure of the concretes formulated and manufactured, as well as the compactness of their granular stacks, in order to predict their impact on their durability.

2. Materials and Methods

The microstructure of the samples was examined and analyzed using a JEOL JSM-6084LV scanning electron microscope (SEM) operating at an acceleration voltage of 10 kV. This high-precision instrument allows for detailed exploration of surface topography by scanning the surfaces with a focused electron beam [5]. The interaction between the incident electrons and the material generates various signals (secondary electrons, backscattered electrons), which are collected to produce

high-resolution images [6].

Therefore, **Figure 1** and **Figure 2** illustrate the surface morphology of the samples, highlighting specific microscopic structures. Thanks to this imaging technique, it was possible to accurately capture fine and subtle details, including topographical irregularities, cracks, pores, and characteristic granular patterns. These observations provide a better understanding of the morphological characteristics inherent in the materials studied. Microscopic analysis reveals a diversity of textures present on the surface of the samples, revealing the existence of distinct structures that may be correlated with their physical, thermal and mechanical properties. These textures include grain alignments, interface zones, surface defects, and local variations in chemical composition, all of which can significantly influence the overall behaviour of the material.

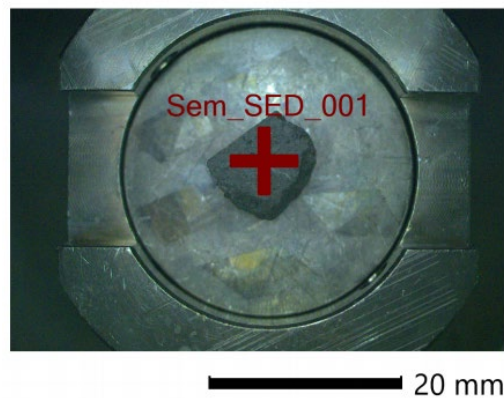


Figure 1. Concrete sample for SEM testing (formulation 1).

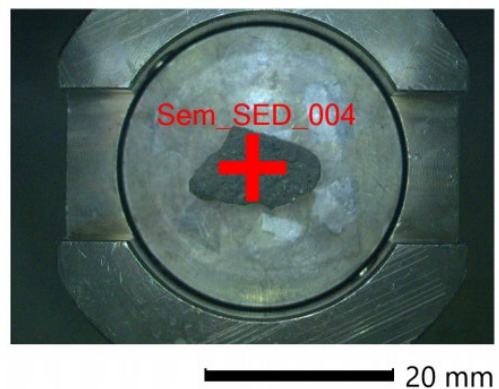


Figure 2. Concrete sample for SEM testing (formulation 4).

Microscopic observations are an essential step in establishing links between the microstructure and functional performance of materials, particularly in specific application contexts such as mechanical strength, thermal conductivity, or long-term durability [7]. This approach thus makes it possible to guide the development of materials optimized for their intended uses.

Presentation of Data

Several laboratory tests were carried out on aggregate samples taken from the cities of Brazzaville and Pointe-Noire, with the aim of developing a varied range of concrete formulations that meet satisfactory rheological criteria. This work also aimed to determine an optimal formulation, taking into account the microstructure and compactness of the matrix. Thus, a balanced particle size distribution was sought during the study phase of the concrete formulation based on the aggregates (sand and gravel) collected. Two types of sand (rolled and crushed) were used to assess the influence of the grain size of the rolled sand, with varying proportions of crushed sand between 30% and 50% [8] [9].

A total of eight (8) concrete formulations were studied using the Dreux-Gorisse method. The corresponding data are presented in **Table 1**. The different formulations differ mainly in the sources and types of aggregates used:

Table 1. Physical and mechanical characteristics of the concretes studied [8].

| Type of concrete formulation | Age of concrete /days | Compressive strength (MPa) | Theoretical density of concrete (g/cm ³) | Actual density of concrete (g/cm ³) | E/C Report | G/S Report | Consistency and Settling (Cm) |
|------------------------------|-----------------------|----------------------------|--|---|------------|------------|-------------------------------|
| Formulation 1 | 7 | 27.75 | 2.37 | 2.38 | 0.49 | 2.45 | Plastic |
| | 28 | 33.75 | | 2.41 | | | 6 |
| Formulation 2 | 7 | 20.50 | 2.38 | 2.37 | 0.49 | 1.80 | Plastique |
| | 28 | 26.65 | | 2.37 | | | 6 |
| Formulation 3 | 7 | 23.85 | 2.37 | 2.42 | 0.49 | 2.43 | Plastique |
| | 28 | 36.75 | | 2.44 | | | 7 |
| Formulation 4 | 7 | 18.10 | 2.37 | 2.41 | 0.49 | 1.70 | Plastique |
| | 28 | 27.25 | | 2.39 | | | 6 |
| Formulation 5 | 7 | 16.50 | 2.36 | 2.25 | 0.47 | 3.06 | Plastique |
| | 28 | 22.80 | | 2.26 | | | 7 |
| Formulation 6 | 7 | 12.60 | 2.35 | 2.22 | 0.47 | 1.70 | Plastique |
| | 28 | 18.30 | | 2.25 | | | 9 |
| Formulation 7 | 7 | 21.50 | 2.38 | 2.37 | 0.49 | 2.36 | Plastique |
| | 28 | 27.30 | | 2.37 | | | 9 |
| Formulation 8 | 7 | 22.10 | 2.37 | 2.36 | 0.49 | 1.89 | Plastique |
| | 28 | 29.70 | | 2.35 | | | 6 |

Formulation 1: Made with a mixture of two grades of crushed gravel (10/14 and 5/15) from the Kombé quarry in Brazzaville, combined with raw sand from the Congo River.

Formulation 2: Identical to formulation 1, but with sand improved by the addition of 50% crushed sand from Inkissi sandstone (Kombé quarry).

Formulation 3: composed of the same crushed gravel as the previous formulations, combined with raw sand from the Mfilou River.

Formulation 4: Similar to formulation 3, but with sand from the Mfilou River enriched with 40% crushed sand.

Formulation 5: Made with a single grade of rolled gravel (3/8) from the Boubissi quarry in Pointe-Noire, as well as local raw sand.

Formulation 6: Similar to formulation 5, but using improved sand composed of 50% crushed sand.

Formulation 7: Made with crushed gravel from the Louvoulou quarry in Pointe-Noire and raw sand from the same region.

Formulation 8: Identical to formulation 7, but with improved sand containing 50% crushed sand.

All of these tests made it possible to identify the most effective grain size combinations in order to optimise the microstructure of the concrete. This optimization contributes to improving the rheological properties while ensuring a homogeneous and consistent structure at the microscopic level.

3. Results and Interpretations

3.1. Formulation 1

Figure 3 and **Figure 4** show observations made using a scanning electron microscope (SEM) at magnifications of $\times 330$ and $\times 1000$, highlighting the continuous structure of the concrete. The SEM images reveal a dense structure, while **Figure 4** shows the presence of large pores on the surface of the sample, providing relevant information on the quality of the concrete analyzed. Furthermore, the chemical composition of the material and the mechanical strength measured at 28 days (33.75 MPa) confirms that this concrete meets the requirements of class C25/30, despite the use of fine sand. This indicates that, even when using materials considered less than optimal, the concrete studied exhibits satisfactory performance and durability. The in-depth chemical analysis not only provided a better understanding of the composition of the concrete, but also identified potential interactions between its various constituents, which can influence its mechanical properties and durability. These results thus provide useful information for optimizing concrete formulations and designing more efficient construction materials. Furthermore, the data from the EDS spectrum of the examined area (presented in **Table 2** and **Figure 5**) reveal a high oxygen content (53.99%), followed by calcium (28.17%), carbon (10.50%) and platinum (2.47%). Other elements are also detected, such as silicon (1.72%), nitrogen (1.39%), as well as traces of iron (0.25%), potassium (0.49%), magnesium (0.17%), Sulphur (0.29%) and aluminium (0.57%). These data enrich our understanding of the chemical composition of concrete and enable a more in-depth analysis of its properties and performances.

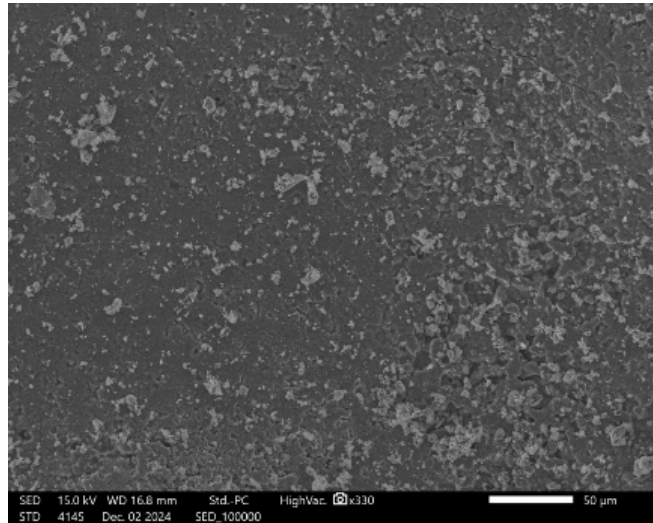


Figure 3. SEM micrograph of the concrete sample magnified at 330.

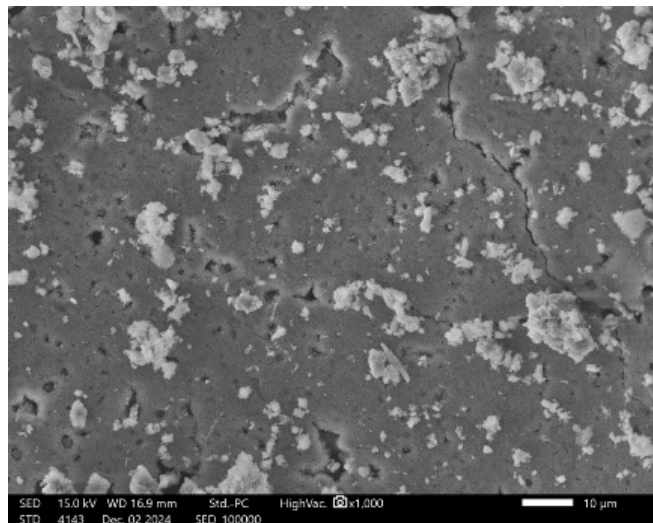
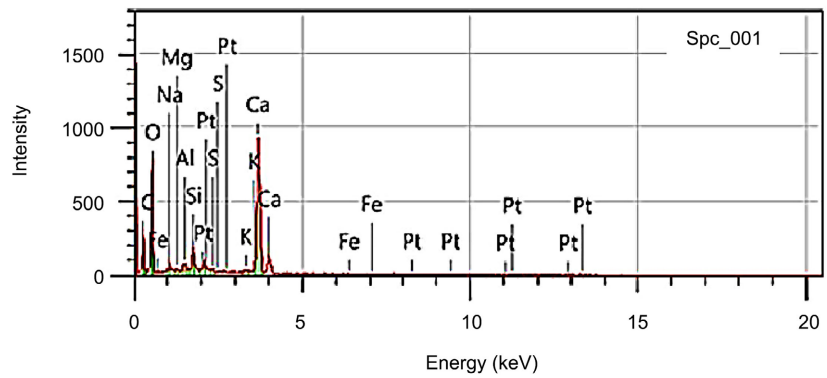


Figure 4. SEM micrograph of the concrete sample magnified 1000 times.



Note. The values of the chemical elements shown in the graphs (Figure 5) are provided in Table 2.

Figure 5. EDS spectrum of the analysed area.

Table 2. EDS analysis results.

| Elements | Weight (%) | Errors (%) |
|----------|--------------|--------------|
| C | 10.50 ± 0.43 | 17.01 ± 0.70 |
| O | 53.99 ± 2.09 | 65.65 ± 2.54 |
| Na | 1.39 ± 0.24 | 1.17 ± 0.20 |
| Mg | 0.17 ± 0.08 | 0.14 ± 0.06 |
| Al | 0.57 ± 0.12 | 0.41 ± 0.09 |
| Si | 1.72 ± 0.19 | 1.19 ± 0.13 |
| S | 0.29 ± 0.08 | 0.17 ± 0.05 |
| K | 0.49 ± 0.12 | 0.24 ± 0.06 |
| Ca | 28.17 ± 0.95 | 13.68 ± 0.46 |
| Fe | 0.25 ± 0.17 | 0.09 ± 0.06 |
| Pt | 2.47 ± 0.39 | 0.25 ± 0.04 |
| Total | 100.00 | 100.00 |
| Spc 001 | | 0.4469 |

3.2. Formulation 2

Microscopic observations (**Figure 6** and **Figure 7**) reveal a compact texture, as well as a concentration and consolidation of aggregates, particularly gravel, grouped together in clusters in the mixture (**Figure 7**). The presence of inter-aggregate pore networks and calcium silicate hydrates (CSH) [10] is also visible in the concrete matrix, these elements becoming more noticeable as the magnification increases. This compact structure, combined with a pore network, directly influences the properties of the concrete. The mechanical strength measured at 28 days is 26.65 MPa, which is lower than that obtained with mixtures containing raw sand, raising questions about the effect of the materials used. The dominant chemical composition, in particular the high presence of oxygen and calcium (see **Table 3** and **Figure 8**), could partly explain this decrease in strength. Nevertheless, it is important to note that the concrete analyzed still has characteristics consistent with C25/30 concrete. This result remains encouraging, especially considering the improvement in the sand used. This shows that, despite certain limitations, the mixture was designed to meet the standard requirements. All of these observations highlight the crucial importance of material selection and formulation in achieving the expected mechanical performance.

3.3. Formulation 3

The images obtained by scanning electron microscopy (SEM) (**Figure 9** and **Figure 10**) reveal a very compact structure, although a few pores are visible in **Figure 10**. The mechanical strength measured at 28 days reached 36.75 MPa, which is fully in line with the expected characteristics for C25/30 concrete. This result confirms the quality of the formulation and the compliance of the mechanical properties with current standards. Furthermore, chemical analysis (**Table 4** and **Figure 11**) shows that the elements present in the concrete had no negative effect on its strength. This

suggests that the use of raw sand from the Mfilou River contributed favorably to the overall performance of the material. In conclusion, these results highlight the decisive role of component selection and formulation in the development of concrete that is both high-performance and durable.

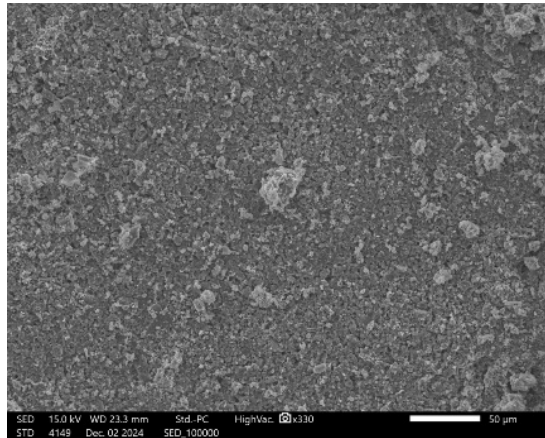


Figure 6. SEM micrograph of the concrete sample magnified at x330.

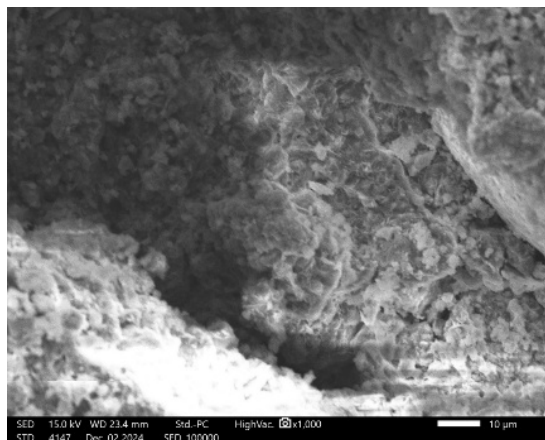
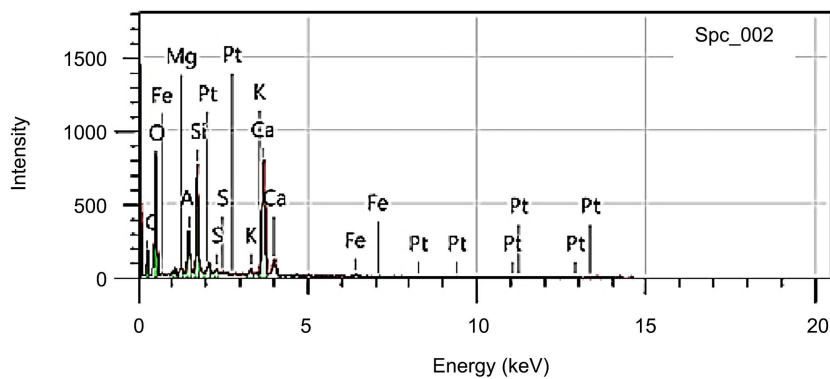


Figure 7. SEM micrograph of the concrete sample magnified 1000 times.

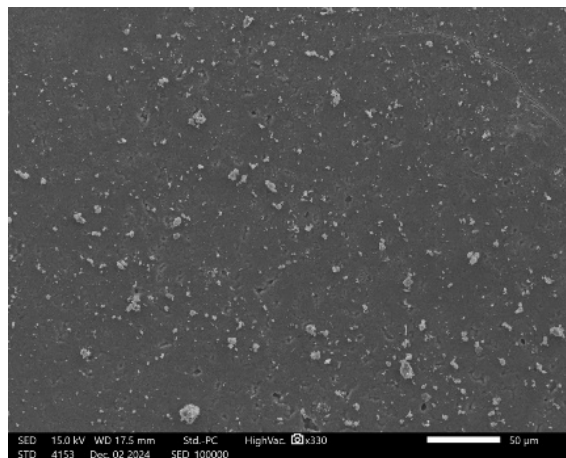
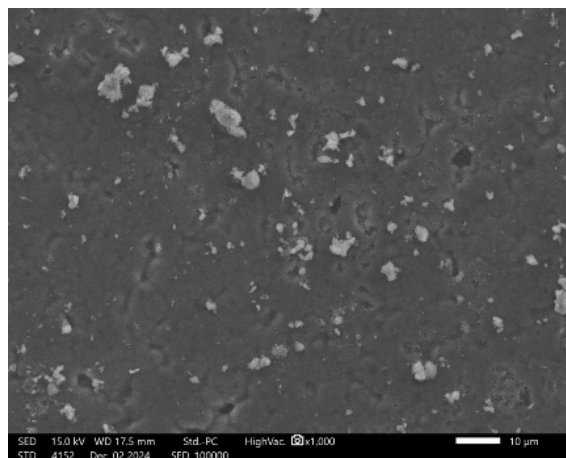


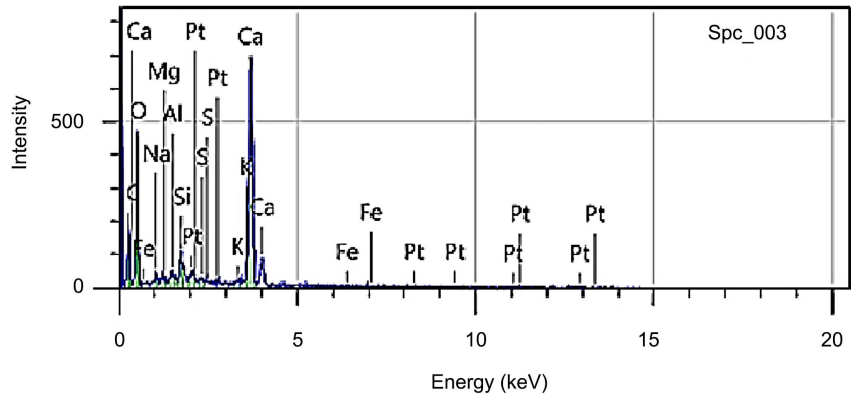
Note. The values of the chemical elements shown in the graphs (Figure 8) are provided in Table 3.

Figure 8. EDS spectrum of the analysed area.

Table 3. EDS analysis results.

| Elements | Weight (%) | Errors (%) |
|----------|--------------|--------------|
| C | 9.95 ± 0.46 | 15.88 ± 0.78 |
| O | 48.91 ± 1.77 | 61.70 ± 2.23 |
| Na | 0.21 ± 0.09 | 0.18 ± 0.08 |
| Mg | 0.29 ± 0.09 | 0.24 ± 0.07 |
| Al | 3.37 ± 0.25 | 2.52 ± 0.19 |
| Si | 8.94 ± 0.40 | 6.42 ± 0.29 |
| S | 0.37 ± 0.09 | 0.23 ± 0.06 |
| K | 0.92 ± 0.15 | 0.47 ± 0.08 |
| Ca | 22.90 ± 0.80 | 11.53 ± 0.40 |
| Fe | 1.32 ± 0.34 | 0.48 ± 0.12 |
| Pt | 3.33 ± 0.42 | 0.34 ± 0.04 |
| Total | 100.00 | 100.00 |
| Spc 002 | | 0.3988 |

**Figure 9.** SEM micrograph of the concrete sample magnified at ×330.**Figure 10.** SEM micrograph of the concrete sample magnified 1000 times.



Note. The values of the chemical elements shown in the graphs (Figure 11) are provided in Table 4.

Figure 11. EDS spectrum of the analysed area.

Table 4. EDS analysis results.

| Elements | Weight (%) | Errors (%) |
|----------|--------------|--------------|
| C | 10.31 ± 0.51 | 16.87 ± 0.84 |
| O | 53.36 ± 2.59 | 65.54 ± 3.18 |
| Na | 0.63 ± 0.20 | 0.54 ± 0.17 |
| Mg | 0.14 ± 0.09 | 0.11 ± 0.07 |
| Al | 0.48 ± 0.14 | 0.35 ± 0.10 |
| Si | 1.40 ± 0.21 | 0.98 ± 0.15 |
| S | 0.28 ± 0.10 | 0.17 ± 0.06 |
| K | 0.36 ± 0.13 | 0.18 ± 0.06 |
| Ca | 30.49 ± 1.20 | 14.95 ± 0.59 |
| Fe | 0.24 ± 0.21 | 0.08 ± 0.07 |
| Pt | 2.31 ± 0.46 | 0.23 ± 0.05 |
| Total | 100.00 | 100.00 |
| Spc 003 | | 0.5139 |

3.4. Formulation 4

The micrographs obtained by scanning electron microscopy (Figure 12 and Figure 13) highlight the presence of aggregates and inter-aggregate porosity, revealing a relatively compact microstructure. The grains are juxtaposed, but numerous voids remain between the aggregates. These images show a network of pores that could negatively affect the strength of the concrete. Indeed, the mechanical strength measured at 28 days is 27.25 MPa, which is lower than expected for formulation 3. The use of improved sand seems to have increased the percentage of inter-aggregate pores in the material, which has contributed to a deterioration in the overall quality of the concrete. Furthermore, chemical analysis (Table 5 and Figure 14) reveals a significant proportion of oxygen and calcium, which warrants particular attention. The high oxygen content could reflect significant chemical

interactions within the mixture, while calcium, a fundamental element in the formation of calcium hydrates, plays a key role in the strength and durability of concrete. These observations provide crucial information for a better understanding of the material's characteristics and its behaviour under various conditions of use.

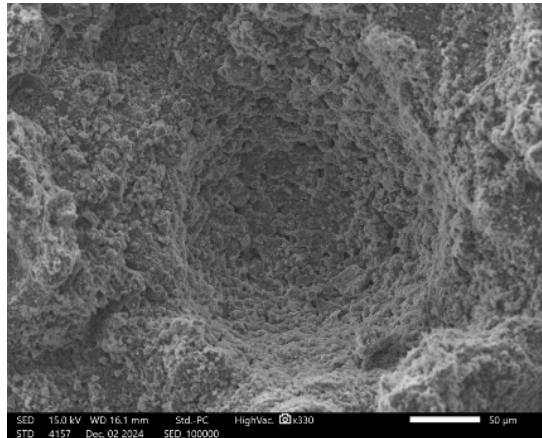


Figure 12. SEM micrograph of the concrete sample magnified at $\times 330$.

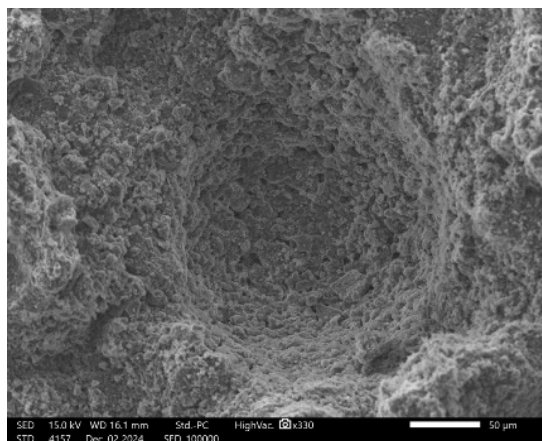
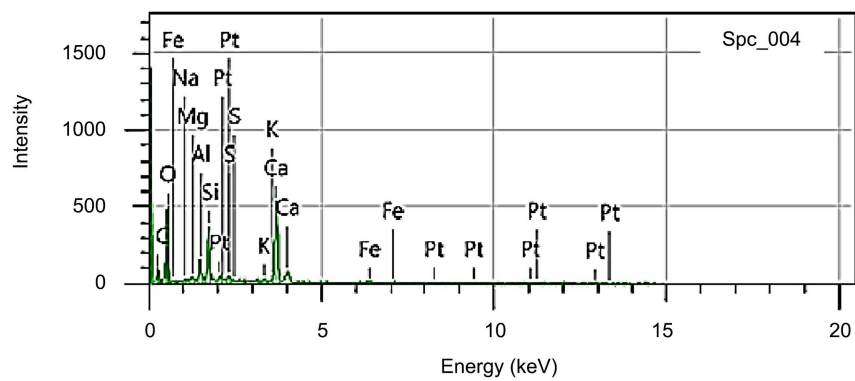


Figure 13. SEM micrograph of the concrete sample magnified 1000 times.



Note. The values of the chemical elements shown in the graphs (Figure 14) are provided in Table 5.

Figure 14. EDS spectrum of the analysed area.

Table 5. EDS analysis results.

| Elements | Weight (%) | Errors (%) |
|----------|--------------|--------------|
| C | 7.60 ± 0.53 | 12.82 ± 0.90 |
| O | 51.11 ± 2.42 | 64.77 ± 3.07 |
| Na | 0.22 ± 0.13 | 0.19 ± 0.11 |
| Mg | 0.48 ± 0.14 | 0.40 ± 0.12 |
| Al | 3.04 ± 0.32 | 2.29 ± 0.24 |
| Si | 7.09 ± 0.48 | 5.12 ± 0.34 |
| S | 0.70 ± 0.15 | 0.44 ± 0.10 |
| K | 0.64 ± 0.17 | 0.33 ± 0.09 |
| Ca | 25.61 ± 1.12 | 12.96 ± 0.57 |
| Fe | 1.22 ± 0.44 | 0.44 ± 0.16 |
| Pt | 2.29 ± 0.47 | 0.24 ± 0.05 |
| Total | 100.00 | 100.00 |
| Spc 004 | | 0.5295 |

3.5. Formulation 5

SEM micrographs (Figure 15 and Figure 16) reveal the presence of aggregates and porosity between them in the sample studied. Large clusters of grains can be seen, accompanied by inter-aggregate voids (Figure 16). The formation of these large aggregates creates empty spaces between them, which contributes to the overall porosity of the material. It is essential to emphasize that this porosity plays a key role in the transition zone of the concrete, causing a weakness in the adhesion between the cement paste and the aggregates. The presence of large, clearly visible pores in the sample appears to be responsible for the reduction in mechanical strength, measured at 22.80 MPa after 28 days. These cavities compromise the structural strength, indicating that this concrete does not meet the requirements of a C25/30 class. This highlights the need to control porosity in order to ensure the required mechanical performance. A high oxygen content is also observed, followed by a significant proportion of calcium (Table 6 and Figure 17). The predominance of oxygen in the chemical composition reflects important characteristics of the concrete, particularly in terms of structure and mechanical properties. Calcium, for its part, is essential for the formation of calcium hydrates, which play a decisive role in the strength and durability of the material. These elements are fundamental for evaluating the performance of concrete in various applications and ensuring its compliance with construction standards.

3.6. Formulation 6

Microscopic observation (Figure 18 and Figure 19) revealed a compact and uni-

form concrete structure. Rolled aggregates can also be seen, with a weak bond between them and the matrix, as well as a network of micropores. The micrographs confirm the dense texture of the concrete, while highlighting the significant presence of pores. This porosity raises concerns, as it directly influences the mechanical strength of the material. Indeed, the strength measured at 28 days, which reaches 18.30 MPa, remains below expectations for high-quality concrete. This suggests that the pores present have a significant impact on the mechanical performance of the concrete. It would therefore be wise to consider solutions to reduce this porosity, such as optimising the composition of the concrete or improving the methods of implementation, in order to achieve the desired performance. Furthermore, chemical analysis of the sample (Table 7 and Figure 20) reveals a high concentration of oxygen, followed by calcium, as in the previous samples.

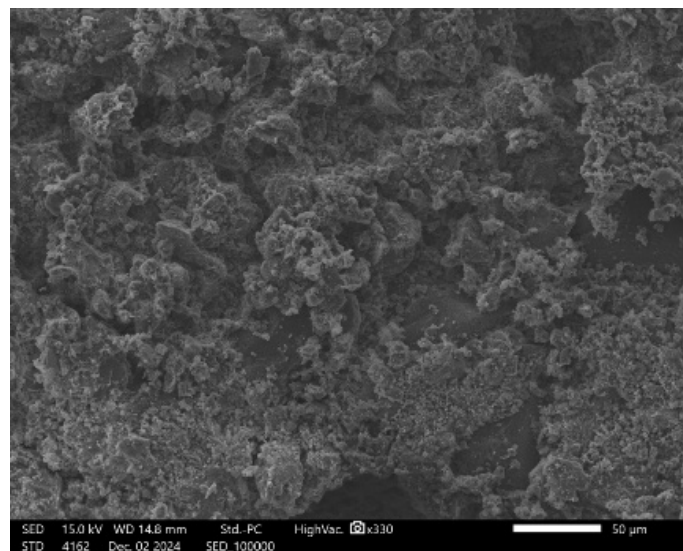


Figure 15. SEM micrograph of the concrete sample magnified at $\times 330$.

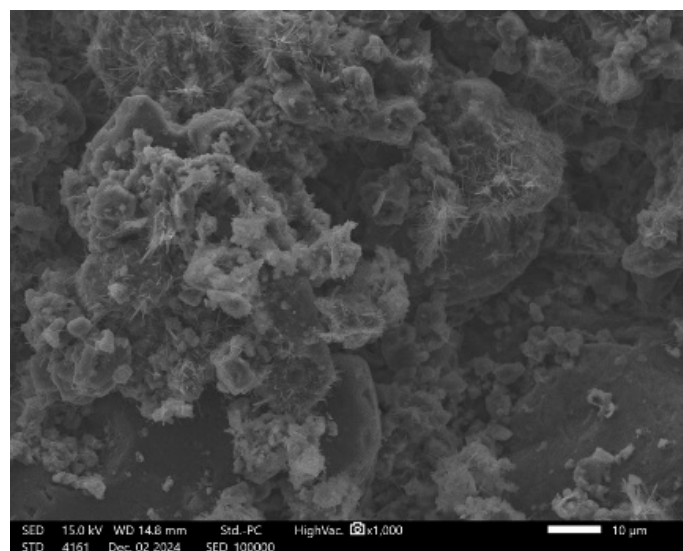
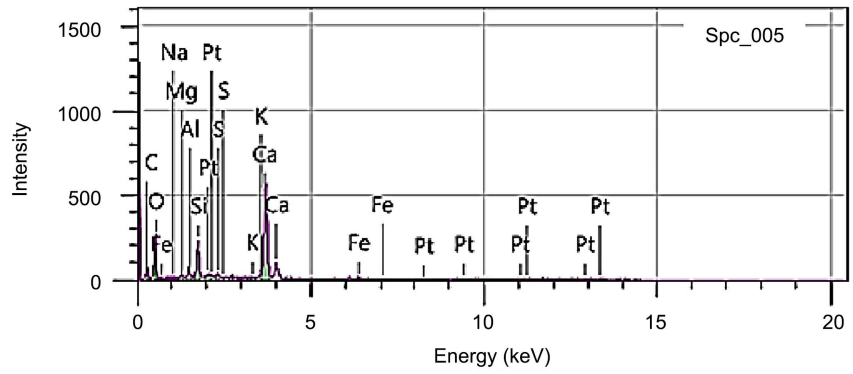


Figure 16. SEM micrograph of the concrete sample magnified 1000 times.



Note. The values of the chemical elements shown in the graphs (Figure 17) are provided in Table 6.

Figure 17. EDS spectrum of the analysed area.

Table 6. EDS analysis results.

| Elements | Weight (%) | Errors (%) |
|----------|--------------|--------------|
| C | 6.21 ± 0.52 | 11.24 ± 0.95 |
| O | 45.51 ± 2.88 | 61.86 ± 3.92 |
| Na | 0.28 ± 0.16 | 0.27 ± 0.15 |
| Mg | 0.63 ± 0.19 | 0.57 ± 0.17 |
| Al | 1.22 ± 0.19 | 0.99 ± 0.19 |
| Si | 5.54 ± 0.48 | 4.29 ± 0.37 |
| S | 0.61 ± 0.17 | 0.41 ± 0.11 |
| K | 0.32 ± 0.14 | 0.18 ± 0.06 |
| Ca | 35.10 ± 1.49 | 19.04 ± 0.81 |
| Fe | 2.30 ± 0.68 | 0.90 ± 0.27 |
| Pt | 2.27 ± 0.54 | 0.25 ± 00.6 |
| Total | 100.00 | 100.00 |
| Spc 005 | | 0.5680 |

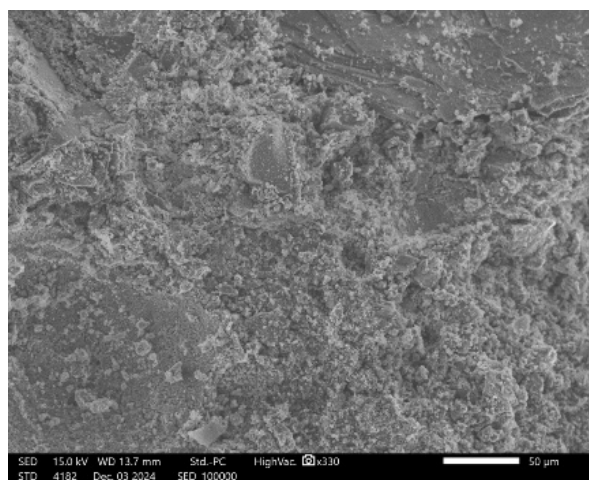


Figure 18. SEM micrograph of the concrete sample magnified at x330.

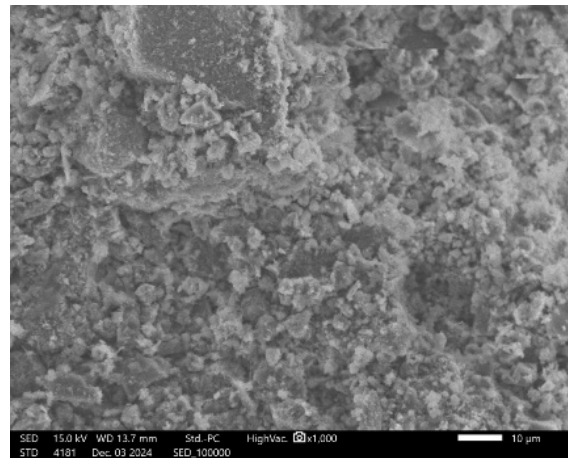
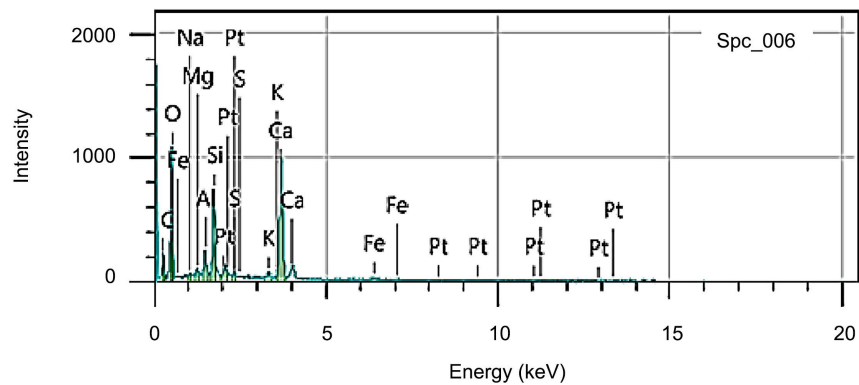


Figure 19. SEM micrograph of the concrete sample magnified 1000 times.



Note. The values of the chemical elements shown in the graphs (**Figure 20**) are provided in **Table 7**.

Figure 20. EDS spectrum of the analysed area.

Table 7. EDS analysis results.

| Elements | Weight (%) | Errors (%) |
|----------|--------------|--------------|
| C | 8.92 ± 0.43 | 14.77 ± 0.70 |
| O | 51.89 ± 1.54 | 64.48 ± 1.92 |
| Na | 0.16 ± 0.08 | 0.14 ± 0.07 |
| Mg | 0.69 ± 0.11 | 0.56 ± 0.09 |
| Al | 2.71 ± 0.21 | 2.00 ± 0.15 |
| Si | 10.56 ± 0.39 | 7.47 ± 0.28 |
| S | 0.54 ± 0.10 | 0.33 ± 0.06 |
| K | 0.56 ± 0.11 | 0.28 ± 0.06 |
| Ca | 18.06 ± 0.34 | 8.96 ± 0.32 |
| Fe | 1.58 ± 0.34 | 0.56 ± 0.12 |
| Pt | 4.34 ± 0.43 | 0.44 ± 0.04 |
| Total | 100.00 | 100.00 |
| Spc 006 | | 0.4072 |

3.7. Formulation 7

Microscopic observation (**Figure 21** and **Figure 22**) reveals a compact and homogeneous structure of the material, which is a favourable indicator of its quality. In addition, networks of pores are observed between the aggregates. The micrographs confirm the dense and firm texture of the concrete, while revealing a network of micropores within the matrix. This microscopic analysis is essential for assessing the quality of the material. The mechanical strength measured at 28 days, amounting to 27.30 MPa, shows that the concrete meets the required performance criteria, which is directly related to its microstructure. Its compliance with class C25/30 also attests to its suitability for common structural uses, guaranteeing sufficient strength for many applications. Finally, the chemical analysis of the sample (**Table 8** and **Figure 23**) provides additional information on the quality and performance of the concrete, highlighting the nature of the elements present.

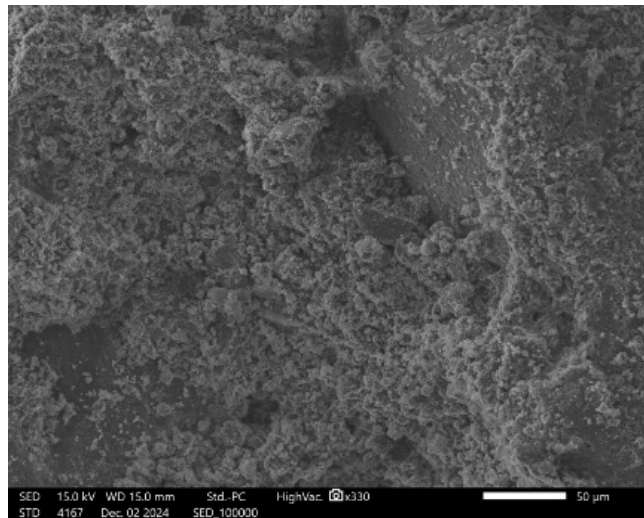


Figure 21. SEM micrograph of the concrete sample magnified at $\times 330$.

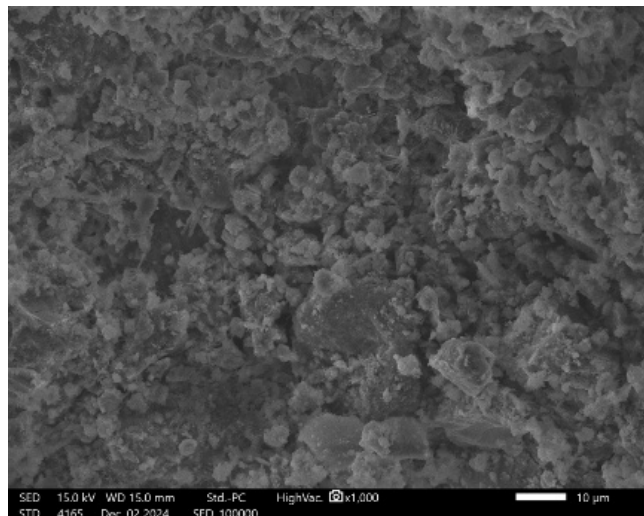
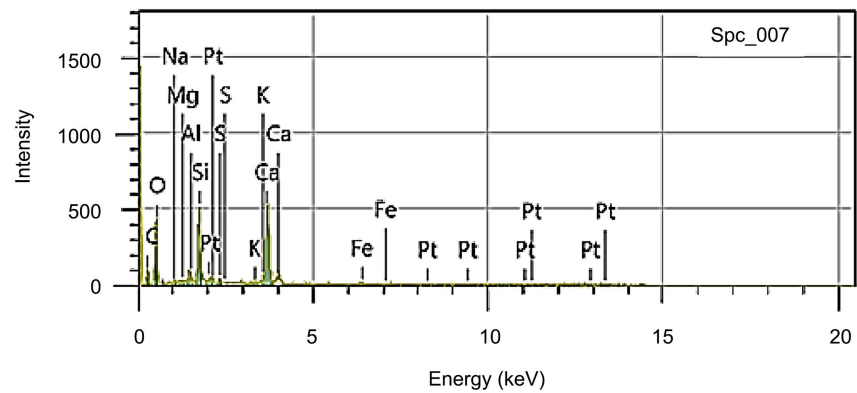


Figure 22. SEM micrograph of the concrete sample magnified 1000 times.



Note. The values of the chemical elements shown in the graphs (Figure 23) are provided in Table 8.

Figure 23. EDS spectrum of the analysed area.

Table 8. EDS analysis results.

| Elements | Weight (%) | Errors (%) |
|----------|--------------|--------------|
| C | 9.17 ± 0.40 | 15.10 ± 0.66 |
| O | 52.34 ± 1.65 | 64.72 ± 2.04 |
| Na | 0.30 ± 0.10 | 0.26 ± 0.09 |
| Mg | 0.66 ± 0.12 | 0.54 ± 0.09 |
| Al | 2.26 ± 0.19 | 1.66 ± 0.14 |
| Si | 7.36 ± 0.33 | 5.18 ± 0.24 |
| S | 0.43 ± 0.09 | 0.27 ± 0.05 |
| K | 0.84 ± 0.13 | 0.42 ± 0.07 |
| Ca | 22.58 ± 0.73 | 11.15 ± 0.36 |
| Fe | 1.19 ± 0.30 | 0.42 ± 0.11 |
| Pt | 2.88 ± 0.36 | 0.29 ± 0.04 |
| Total | 100.00 | 100.00 |
| Spc 007 | | 0.4116 |

3.8. Formulation 8

The micrographs (Figure 24 and Figure 25) show a dense and compact concrete texture, accompanied by a network of micropores, which is a determining factor in their performance. The mechanical strength obtained at 28 days, which is 29.70 MPa, demonstrates the good quality of the material, which is closely linked to its microstructure. This strength is a key indicator for assessing the durability and reliability of concrete in structural applications. Furthermore, the conformity of this concrete with class C25/30 confirms that it meets the normative requirements for a wide range of constructions, thus ensuring its ability to withstand significant

structural loads. The chemical analysis (Table 9 and Figure 26) provides additional information on the mechanical properties of the material, revealing the nature of the elements present.

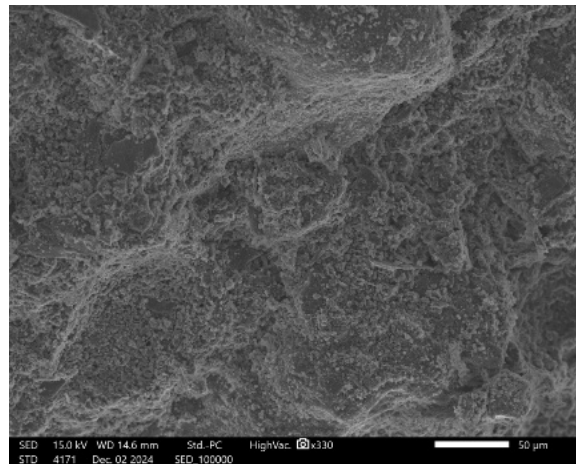


Figure 24. SEM micrograph of the concrete sample magnified at ×330.

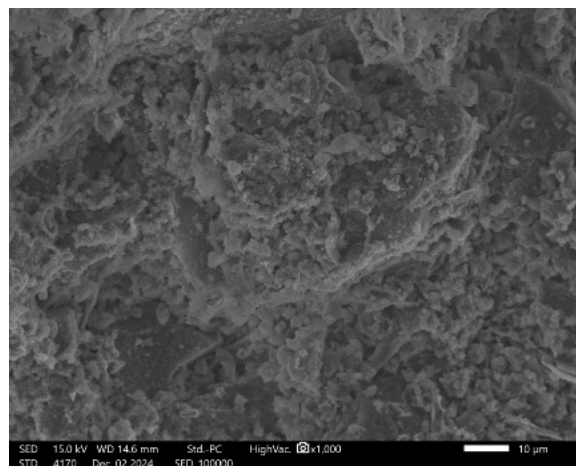
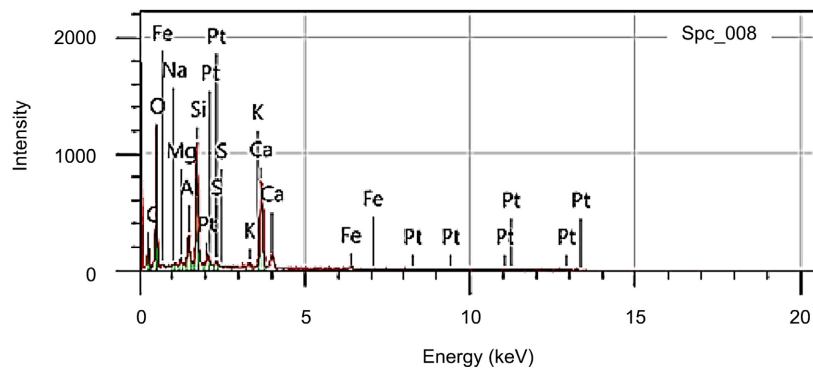


Figure 25. SEM micrograph of the concrete sample magnified 1000 times.



Note: The values of the chemical elements shown in the graphs (Figure 26) are provided in Table 9.

Figure 26. EDS spectrum of the analysed area.

Table 9. Results of the EDS analysis.

| Elements | Weight (%) | Errors (%) |
|----------|--------------|--------------|
| C | 7.76 ± 0.56 | 13.32 ± 0.96 |
| O | 48.86 ± 2.42 | 62.96 ± 3.12 |
| Na | 0.21 ± 0.12 | 0.19 ± 3.12 |
| Mg | 0.46 ± 0.14 | 0.39 ± 0.12 |
| Al | 1.51 ± 0.23 | 1.16 ± 0.18 |
| Si | 9.56 ± 0.55 | 7.02 ± 0.40 |
| S | 0.68 ± 0.16 | 0.44 ± 0.10 |
| K | 0.36 ± 0.13 | 0.19 ± 0.07 |
| Ca | 26.22 ± 1.14 | 13.49 ± 0.59 |
| Fe | 1.49 ± 0.49 | 0.55 ± 0.18 |
| Pt | 2.88 ± 0.53 | 0.30 ± 0.06 |
| Total | 100.00 | 100.00 |
| Spc 008 | | 0.5330 |

4. Discussion

Several authors have already worked on the microstructural characterisation of concrete. Researchers such as Elat *et al.* (2021), Sawssen *et al.* (2017), Sachet *et al.* (2013), and Li *et al.* (2020) have demonstrated the importance of this topic by highlighting the significance of the physical and mechanical properties of materials for concrete formulation and their impact on its microstructure.

That being said, in the context of our work, the energy dispersive spectrometer (EDS) system has effectively provided valuable elemental images for analysing the chemical composition of concrete samples. By examining the eight samples from Brazzaville and Pointe-Noire, it was possible to identify various chemical elements, including carbon (C), oxygen (O), sodium (Na), magnesium (Mg), aluminium (Al), silicon (Si), sulphur (S), potassium (K), calcium (Ca), iron (Fe) and platinum (Pt).

The results show a predominance of oxygen, calcium and carbon in all samples, which is consistent with the structure of cementitious materials. The high presence of oxygen is particularly linked to the micropores present in concrete, which influence its mechanical properties.

However, concrete made with washed sand has slightly higher oxygen, calcium and carbon content than concrete made with 50% improved sand. In Brazzaville, concrete formulations using raw or improved sand comply with C25/30 standards, but concrete made with raw sand shows better mechanical strength at 28 days.

The microstructure observed under SEM reveals a compact texture with no preferential grain orientation, but with micropores, which may explain the lower strength of concretes based on improved sand.

For the Pointe-Noire locality, SEM observations also indicate compact and homogeneous structures, but with low adhesion at the matrix level, as well as a network of pores and micropores. Formulations 5 and 6 do not meet C25/30 standards, while formulations 7 and 8 do.

In summary, the microstructure and chemical composition of concrete play a crucial role in its mechanical performance, and the differences observed between locations and types of sand used highlight the importance of these factors in the design of high-quality concrete [11].

Nevertheless, microstructural studies conducted by Sawssen *et al.* [12] have demonstrated that porosity plays a fundamental role in the transition zone of concrete, as it directly influences the quality of adhesion between the cement paste and the aggregates. High porosity leads to a decrease in cohesion between these two phases, which can weaken the overall structure of the concrete and reduce its load-bearing capacity. This observation is essential, as it highlights the need to optimise the compactness of concrete in order to improve its mechanical performance.

These results confirm that the decrease in strength of the concretes studied can be mainly attributed to the quality of the bond between the cement paste and the aggregates. Insufficient adhesion in this critical area leads to increased fragility of the material and promotes the appearance of microcracks under the effect of applied loads. This trend was observed in the experimental results of compressive strength for the different formulations analysed in the study. Similarly, Sachet *et al.* [13] emphasised that porosity is a determining factor in the evaluation of the mechanical performance of concrete. The higher the porosity of a concrete, the weaker the cement matrix, which results in a significant decrease in its mechanical strength. Indeed, a porous structure facilitates the propagation of cracks and reduces the durability of concrete when subjected to mechanical stresses and external aggressions. This relationship between porosity and mechanical strength was clearly observed in formulations 2, 4, 5 and 6 of the study. These formulations had higher porosity than the others, which directly compromised their compressive strength. This phenomenon can be explained by poor aggregate distribution, an excess of fines, or an inappropriate water/cement ratio, leading to a less dense and therefore more vulnerable structure. Thus, microstructural analysis reinforces the idea that controlling porosity is an essential lever for improving the quality and durability of concrete.

Elat [14], using SEM analysis, confirmed the crucial role of porosity in concrete structure. His research highlighted an increased presence of microcracks in mortars composed solely of river sand, compared to those incorporating a balanced mixture of 50% river sand and 50% crushed sand. These results are consistent with the trends observed in the mechanical performance of the different formulations studied, suggesting that the particle size distribution directly influences the strength and durability of concrete.

In addition, Elat carried out an in-depth chemical analysis, revealing significant

differences between river sand and crushed sand. River sand has a high silicon (Si) and oxygen (O) content, with concentrations significantly higher than in crushed sand. On the other hand, crushed sand has higher levels of magnesium (Mg), aluminium (Al), potassium (K), iron (Fe) and sodium (Na). These chemical variations can explain certain differences in the mechanical performance and durability of concrete, due to their effects on the reaction of the cement paste and the formation of hydration products.

The importance of microstructural characteristics in concrete performance was also highlighted by Li *et al.* [15]. They demonstrated that optimising the particle size distribution, taking into account both porosity and chemical interactions, contributes significantly to improving the compressive strength and durability of concrete. These observations are consistent with the results obtained in Brazzaville, where it was found that the use of well-calibrated substitute sands, combined with a reduction in excessive fines, limits the development of microcracks and improves the overall performance of concrete.

Furthermore, research conducted by Elat and Li confirms that controlling the microstructural and chemical parameters of aggregates is a key factor in the design of durable and high-performance concrete. The judicious combination of different types of sand and precise control of their composition optimises the density of the cement matrix, thereby reducing porosity and strengthening the mechanical resistance of the final material.

The results highlight that the choice and combination of aggregates must be carried out with great rigour in order to guarantee optimal mechanical performance and durability of the concrete. Indeed, the microstructural properties of aggregates, such as their porosity, particle size, shape and chemical composition, directly influence the compressive strength, permeability and long-term durability of the material. Excessive porosity can promote the penetration of water and aggressive agents, thereby accelerating degradation phenomena such as cracking, chemical alteration or the development of harmful reactions such as alkali-silica reaction.

The approach adopted in formulations 2 and 4 illustrates the importance of a judicious balance between river sand and crushed sand. River sand, which is generally rounded and low in fines, contributes to good workability of the mixture, while crushed sand, with its more angular grains and rough surface, improves adhesion with the cement paste and strengthens the cohesion of the concrete [16]. A controlled combination of these two types of sand thus optimises the compactness of the material, ensures better mechanical strength and increases durability in the face of environmental stresses and repeated mechanical stresses.

The results highlight the fact that the choice and combination of aggregates must be made with care. The microstructural properties of aggregates, particularly their porosity and chemical composition, play a key role in the mechanical strength and durability of concrete. The approach adopted in formulations 2 and 4 illustrates the importance of striking the right balance between river sand and

crushed sand in order to optimise structural and durability performance.

5. Conclusion

The results obtained in this study highlighted the porous structure of the concrete analysed, characterised by the presence of micropores and larger pores in some samples. These observations underscore the complexity of the internal composition of concrete, which can influence its mechanical properties and durability. In addition, the analyses revealed the presence of a variety of chemical elements in the concretes, including carbon (C), oxygen (O), sodium (Na), magnesium (Mg), aluminium (Al), silicon (Si), sulphur (S), potassium (K), calcium (Ca), iron (Fe) and platinum (Pt). These chemical analyses showed a marked predominance of oxygen (O), calcium (Ca) and carbon (C) in all the samples studied, with significantly higher peak heights for oxygen and carbon, indicating their relative abundance in the composition of the concrete. In addition, silicon (Si) also stands out for its notable presence in samples from the Pointe-Noire area, which could have implications for the specific properties of concrete in this region. The presence of oxygen in concrete is mainly attributed to the porosity of the concrete matrix, which allows air to infiltrate and be retained, thus influencing the physical and chemical characteristics of the material. These results pave the way for a better understanding of the interactions between the chemical composition and properties of concrete, which is essential for optimising its performance in various applications in the civil engineering and construction industries.

Conflicts of Interest

The authors declare no conflicts of interest regarding the publication of this paper.

References

- [1] Philippi, P.C., Yunes, P.R., Fernandes, C.P. and Magnani, F.S. (1994) The Microstructure of Porous Building Materials: Study of a Cement and Lime Mortar. *Transport in Porous Media*, **14**, 219-245. <https://doi.org/10.1007/bf00631003>
- [2] Narcisse, M. (2014) Problème de stockage de l'eau à usage domestique dans les réservoirs en béton armé enterrés sous un sol humide et pollué dans la ville de Brazzaville: Modélisation de la diffusion non linéaire en milieu poreux. Ph.D. Thesis, Université Marien N'gouabi, Congo-Brazzaville.
- [3] Liu, R., Chi, Y., Chen, S., Jiang, Q., Meng, X., Wu, K., et al. (2020) Influence of Pore Structure Characteristics on the Mechanical and Durability Behavior of Pervious Concrete Material Based on Image Analysis. *International Journal of Concrete Structures and Materials*, **14**, Article No. 29. <https://doi.org/10.1186/s40069-020-00404-1>
- [4] Zhang, Y., Xu, S., Fang, Z., Zhang, J. and Mao, C. (2020) Permeability of Concrete and Correlation with Microstructure Parameters Determined by ¹H NMR. *Advances in Materials Science and Engineering*, **2020**, Article ID: 4969680. <https://doi.org/10.1155/2020/4969680>
- [5] Goldstein, J.I., Newbury, D.E., Echlin, P., Joy, D.C., Lyman, C.E., Lifshin, E., Sawyer, L. and Michael, J.R. (2003) *Electron Guns, Scanning, Electron Microscopy and X-Ray Microanalysis*. 3rd Edition, Plenum Press, 29-40.

- [6] Brisset, F. and Ruste, J. (2024) Microscopie électronique à balayage—Principe et équipement. *Techniques d'analyse*. <https://doi.org/10.51257/a-v4-p865>
- [7] Azizi, N. and Mahmudi, R. (2021) Microstructure, Texture, and Mechanical Properties of the Extruded and Multi-Directionally Forged Mg-xGd Alloys. *Materials Science and Engineering: A*, **817**, Article ID: 141385. <https://doi.org/10.1016/j.msea.2021.141385>
- [8] Makela, J.B., Ebata-Ndion, B., Malanda, N. and Mbeke, S.K. (2025) Prospective Study and Physico-Mechanical Characterisation of Granular Materials Used in the Manufacture of Ordinary Concrete in Congo. *Geomaterials*, **15**, 1-24. <https://doi.org/10.4236/gm.2025.151001>
- [9] Malanda, N., Louzolo-Kimbembe, P., Ahouet, L., Makela, J.B. and Mouengue, G. (2019) Concrete Formulation Study for Informal and Semi-Informal Construction Sectors. *Open Journal of Civil Engineering*, **9**, 57-79. <https://doi.org/10.4236/ojce.2019.91005>
- [10] Tran, T.D. (2014) Rôle de la microstructure des sols argileux dans les processus de retrait-gonflement: De l'échelle de l'éprouvette à l'échelle de la chambre environnementale. Ph.D. Thesis, École nationale supérieure des mines de Paris.
- [11] Mehta, P.K. and Monteiro, P.J.M. (2014) Concrete: Microstructure, Properties, and Materials. 4th Edition, McGraw-Hill Education.
- [12] El Euch Ben Saïd, S., El Euch Khay, S. and Loulizi, A. (2017) Compréhension du comportement mécanique du béton de fraisat à travers des observations microscopiques. Institut supérieur des études technologiques, ISET de Radès, Université de Tunis El Manar, LR-MOED-ENIT.
- [13] Sachet, T., Balbo, J.T. and Bonsembiante, F.T. (2013) Rendering the Loss of Strength in Dry Concretes with Addition of Milled Asphalt through Microscopic Analysis. *Revista IBRACON de Estruturas e Materiais*, **6**, 933-954. <https://doi.org/10.1590/s1983-41952013000600006>
- [14] Moukete Emmanuel, E.A. (2021) Formulation, microstructure, durabilité et comportement mécanique du béton à base de carrière combiné au sable alluvion-naire. Thèse de doctorat, Université de CY Cergy.
- [15] Zhu, L., Wang, J., Li, X., Zhao, G. and Huo, X. (2020) Experimental and Numerical Study on Creep and Shrinkage Effects of Ultra High-Performance Concrete Beam. *Composites Part B: Engineering*, **184**, Article ID: 107713. <https://doi.org/10.1016/j.compositesb.2019.107713>
- [16] Tiegoum Wembe, J., Mambou Ngueyep, L.L., Elat Assoua Moukete, E., Eslami, J., Pliya, P., Ndjaka, J.B., *et al.* (2023) Physical, Mechanical Properties and Microstructure of Concretes Made with Natural and Crushed Aggregates: Application in Building Construction. *Cleaner Materials*, **7**, Article ID: 100173. <https://doi.org/10.1016/j.clema.2023.100173>